Efficient Quantum Memory Using a Weakly Absorbing Sample

Mahmood Sabooni, Qian Li, Stefan Kröll, and Lars Rippe
Department of Physics, Lund University, P. O. Box 118, SE-22100 Lund, Sweden
(Received 29 December 2012; published 26 March 2013)

A light-storage experiment with a total (storage and retrieval) efficiency $\eta = 56\%$ is carried out by enclosing a sample, with a single-pass absorption of 10%, in an impedance-matched cavity. The experiment is carried out using the atomic frequency comb (AFC) technique in a praseodymium-doped crystal ($0.05\%Pr^{3+}:Y_2SiO_5$) and the cavity is created by depositing reflection coatings directly onto the crystal surfaces. The AFC technique has previously by far demonstrated the highest multimode capacity of all quantum memory concepts tested experimentally. We claim that the present work shows that it is realistic to create efficient, on-demand, long storage time AFC memories.

DOI: 10.1103/PhysRevLett.110.133604 PACS numbers: 42.50.Ct, 03.67.Hk, 42.50.Gy, 42.50.Md

A quantum memory that has the ability to map onto, store in, and later retrieve the quantum state of light from matter is an important building block in quantum information processing [1]. Quantum memories are expected to become vital elements for long distance quantum key distribution [2,3]. Quantum computing based on linear optics schemes [4], signal synchronization in optical quantum processing [5,6], the implementation of a deterministic single-photon source [7], and precision measurements based on mapping of the quantum properties of an optical state to an atomic ensemble [8] are other applications of quantum memories. For most of the applications mentioned, high performance will be required in terms of high efficiency [9,10], on-demand readout, long storage time [11,12], multimode storage capacity [13,14], and broad bandwidth [15].

Many protocols have been proposed to realize an efficient quantum memory; these include electromagnetically induced transparency (EIT) [16], off-resonant Raman interactions [17], controlled reversible inhomogeneous broadening (CRIB) [18–20], gradient echo memory (GEM) [21], and atomic frequency combs (AFC) [22]. The most impressive storage and retrieval efficiencies so far, 87% [9] and 69% [10], were achieved in hot atomic vapor and rare-earth doped crystals, respectively, using the GEM technique. Additionally, 43% storage and retrieval efficiency using EIT in a hot Rb vapor [23] and 35% using AFC in a rare-earth doped crystal [24] were attained.

The AFC technique [22] is employed in this Letter because the number of (temporal) modes that can be stored in a sample is independent of the optical depth (d) of the storage material, in contrast to other quantum memory approaches. An AFC structure consists of a set of (artificially created) narrow absorbing peaks with equidistant frequency spacing Δ and uniform peak width γ (see the inset in Fig. 3). An input (storage) field (at time $t = 0$) that spectrally overlaps the AFC structure will be absorbed and leave the absorbers (in our case the Pr ions) in a superposition state [22]. If the coherence time is long compared to $1/\Delta$, a collective emission due to constructive interference (similar as for the modes in a mode-locked laser) will occur at time $t_{\text{echo}} = 1/\Delta$.

High storage and retrieval efficiency is one of the main targets of quantum memories and this relies on strong coupling between light and matter [1]. One approach for studying light-matter interaction is based on the high finesse cavity-enhanced interaction of light with a single atom [25,26]. Another alternative for increasing the coupling efficiency of a quantum interface between light and matter is using an optically thick free space atomic ensemble [1]. In this Letter, we combine the advantages of both approaches to implement an efficient quantum interface in a weakly absorbing solid state medium [27]. Within the ensemble approach several experimental realizations from room-temperature alkali gases [28], to alkali atoms cooled and trapped at temperature of a few tens or hundreds of microkelvin [29] have been investigated. Among the ensemble-based approaches impurity centers in a solid state crystal is a powerful alternative for quantum memories because of the absence of atomic movement.

The objective of this Letter is to demonstrate a quantum memory with high storage and retrieval efficiency, with the added benefit of being achievable in a weakly absorbing medium. Another benefit is the short crystal length (2 mm), and small physical storage volume ($\ll \text{mm}^3$). This can simplify the implementation of long-term storage in the hyperfine levels, as will be further discussed at the end of the Letter. For an AFC memory with no cavity and with emission in the forward direction, the maximum theoretical efficiency is limited to 54% [22]. Our work is based on the proposals in Refs. [30,31], where it is shown that close to unity storage and retrieval efficiency can be obtained, using an atomic ensemble in an impedance-matched cavity. A cavity can be impedance matched, by having the absorption per cavity round trip ($1 - e^{-2\alpha L}$) equal to the transmission of the input coupling mirror ($1 - R1$), while the back mirror is 100% reflecting, which gives $R1 = e^{-2\alpha L}$, where α is the absorption coefficient and L is the

length of the optical memory material. For this impedance-matching condition, all light sent to the cavity will be absorbed in the absorbing sample inside the cavity and no light is reflected.

The storage cavity is made up of a 2 mm long 0.05% Pr^{3+}:Y_2SiO_5 crystal; see Fig. 1. To reduce the complexity of the alignment and reduce losses, the crystal surfaces are reflection coated directly, rather than using separate mirrors. The two cavity crystal surfaces are not exactly parallel as shown in Fig. 1 ($\theta \approx 10$ arcsec). Part of the incoming field $\vec{E}_{\rm in}$ will be reflected ($\vec{E}_{\rm refl}$) at the first mirror surface ($R1$), see Fig. 1. The field leaking out through $R1$ from the cavity, $\vec{E}_{\rm leak}$, is coherently added to $\vec{E}_{\rm refl}$ such that $\vec{E}_{\rm out} = \vec{E}_{\rm refl} + \vec{E}_{\rm leak}$. At the impedance-matched condition, $\vec{E}_{\rm refl}$ and $\vec{E}_{\rm leak}$ differ in phase by π and have the same amplitude $|\vec{E}_{\rm refl}| = |\vec{E}_{\rm leak}|$. This means that the light intensity at the reflection detector (PD3) should ideally vanishes if this condition is satisfied.

The cavity crystal (impedance matching) was first tested without memory preparation. The effective cavity length can be optimized by translating the cavity perpendicular to the beam propagation direction. Here a sub-μm accuracy (Attocube system, ANCz150) translation stage was used. Then, a weak Gaussian pulse ($\tau_{\rm FWHM} = 250$ ns) with a small pulse area and repetition rate of 10 Hz was injected into the cavity while the laser frequency was slowly scanned during ~6 s across the inhomogeneous Pr ion absorption line. To find the best impedance-matched point, the cavity crystal was translated in small steps perpendicular to the beam direction. For each step a 18 GHz laser scan was carried out. The calibrated reflected part of the input pulse (PD3/PD1) is plotted versus the frequency offset from the Pr^{3+}:Y_2SiO_5 inhomogeneous line center in Fig. 2, for the position where the highest absorption was obtained. This measurement shows that a maximum of about 84% of the input energy could be absorbed. This occurred about 45 GHz above the inhomogeneous broadening center frequency. This will set an upper limit for the achievable storage and retrieval efficiency in the present setup. Due to the absorption tailoring during the memory preparation (to be discussed below), the impedance-matching condition will be fulfilled closer to the inhomogeneous line center in the actual storage experiment, but the measurement establish the losses caused by spatial mode mismatching. In addition, in the present setup the dye laser is frequency stabilized against a Fabry-Pérot cavity using the Pound-Drever-Hall (PDH) locking technique [32,33]. This provide more freedom for locking the laser frequency further away from the inhomogeneous profile center compared to our earlier work [34] where stabilization based on hole burning was used. This has a

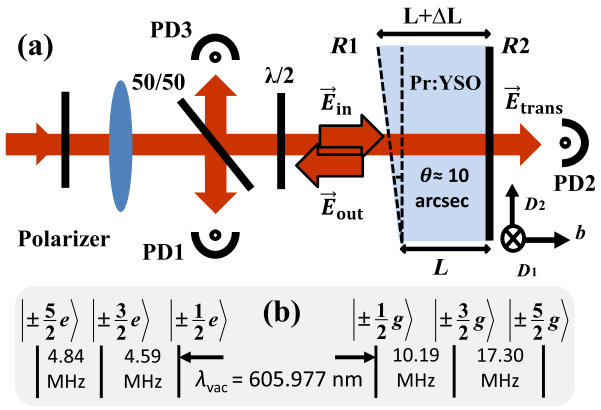

FIG. 1 (color online). (a) Part of the experimental setup. A frequency stabilized (< 1 kHz linewidth) dye laser at $\lambda_{\rm vac} = 605.977$ nm is employed as light source. A 50/50 beam splitter splits off part of the input light onto a photo diode (PD1), to calibrate against variations in the input light intensity. Two other photo diodes monitor the transmitted (PD2) and the reflected (PD3) light from the cavity. The cavity length along the b axis is $L = 2$ mm and the crystal diameter in the (D_1, D_2) plane is 12 mm. b, D_1, and D_2 are principal axes of the crystal [46]. A beam waist of about 100 μm is created at the crystal center via a lens with $f = 400$ mm. A half-wave plate ($\lambda/2$) is employed to align the polarization direction to a principal axis of the cavity crystal, which is immersed in liquid helium at 2.1 K. The input and output facet of the crystal has $R1 = 80\%$ and $R2 = 99.7\%$ reflectivity. A small part of the cavity crystal is left uncoated for measurements without a cavity effect. (b) The hyperfine splitting of the ground $|g\rangle$ and excited $|e\rangle$ state of the $^3H_4 - {}^1D_2$ transition of site I in Pr^{3+}:Y_2SiO_5 [38].

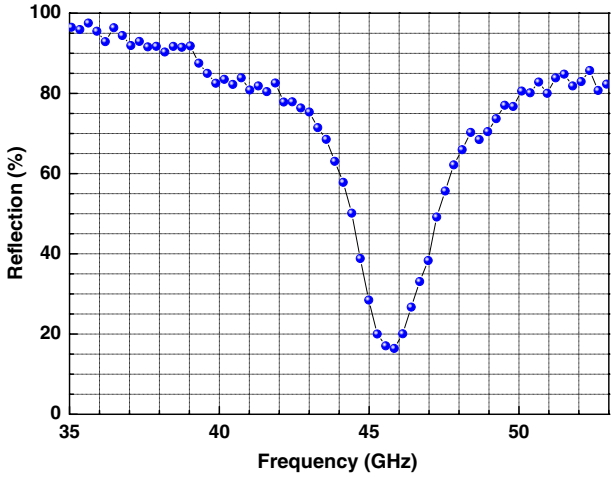

FIG. 2 (color online). The normalized reflected signal (PD3/PD1) is plotted against the frequency offset from the Pr^{3+}:Y_2SiO_5 inhomogeneous line center. The crystal was translated perpendicular to the input beam (see Fig. 1) and the graph is a frequency scan for the position that gave the best impedance matching. At the impedance-matching condition the reflected light detected at PD3 should vanish. The best impedance-matched condition without memory preparation (i.e., spectral manipulation by the absorption profile, see text) was a reflection of 16% (84% absorption), which was measured about 45 GHz above the inhomogeneous broadening center frequency that is located at 0 GHz in this figure.

large influence on improving the impedance-matching condition.

To demonstrate a quantum memory based on the AFC protocol, first, a transparent (nonabsorbing) spectral transmission window within the Pr ion absorption profile was created using optical pumping. An accurate description of the pulse sequences required for creating such a transparency window, which henceforth is called a spectral pit, is given in Ref. [24]. Because of the strong dispersion created by the spectral pit [35], the cavity free spectral range (FSR) and the cavity linewidth are reduced by 3–4 orders of magnitude [36]. The reduction can be understood as follows. The cavity FSR is $\Delta\nu_{\mathrm{mode}} = \frac{c_0}{2L}\frac{1}{n_g}$ [37] where c_0 is speed of light in the vacuum, L is the cavity length, and n_g is the group refractive index. $n_g = n_r(\nu) + \nu\frac{dn_r(\nu)}{d\nu}$ and $n_r(\nu)$ is the real refractive index as a function of frequency ν. In case of no or constant absorption, the dispersion term is negligible compared to the real refractive index ($n_r(\nu) \gg \nu\frac{dn_r(\nu)}{d\nu}$). The FSR of this cavity with no absorbing material is about 40 GHz. In the presence of sharp transmission structures ($n_r(\nu) \ll \nu\frac{dn_r(\nu)}{d\nu}$) a dramatic reduction of the cavity FSR and the cavity linewidth can occur. In our case $\nu\frac{dn_r(\nu)}{d\nu} > 1000 n_r(\nu)$ and the reduction is >3 orders of magnitude at the center of the inhomogeneous line. A more detailed description of the cavity FSR reduction is given in Refs. [34,36]. Translating the crystal perpendicular to the beam propagation direction will move the cavity transmission within the spectral pit due to the small wedge on the crystal.

After preparing the transparent (nonabsorbing) spectral transmission window, each AFC peak is created using a complex hyperbolic secant pulse (sechyp for short) with chirp width $f_{\mathrm{width}} = 70$ kHz [38] and temporal width $t_{\mathrm{FWHM}} = 16.8\ \mu$s [38]. This pulse excites ions from $|\pm\frac{1}{2}g\rangle \mapsto |\pm\frac{5}{2}e\rangle$ state [see Fig. 1(a)]. From the $|\pm\frac{5}{2}e\rangle$ state, Pr ions will decay mostly to the $|\pm\frac{5}{2}g\rangle$ due to the high branching ratio for the $|\pm\frac{5}{2}e\rangle \mapsto |\pm\frac{5}{2}g\rangle$ transition [39]. This pulse is repeated several (~ 50) times with a waiting time of 500 μs between each pulse. This process creates one AFC peak. Repeating this procedure with a consecutive change of center frequency of the sechyp pulse by Δ will create the other AFC peaks. The finesse of the AFC structure with peak width γ and peak separation Δ will be $F_{\mathrm{AFC}} = \frac{\Delta}{\gamma}$.

As we discussed earlier, the absorption engineering of the Pr ions inside the cavity will directly affect the cavity modes via strong dispersion. Therefore, measuring the AFC structure properties in the cavity case is challenging. In order to at least to some extent estimate the AFC structure properties, the coating of a small part of the cavity crystal is removed, and the same preparation as for the memory is performed in this part. The remaining coating could affect the precision of this measurement through the cavity dispersion effect. The trace in Fig. 3 is recorded

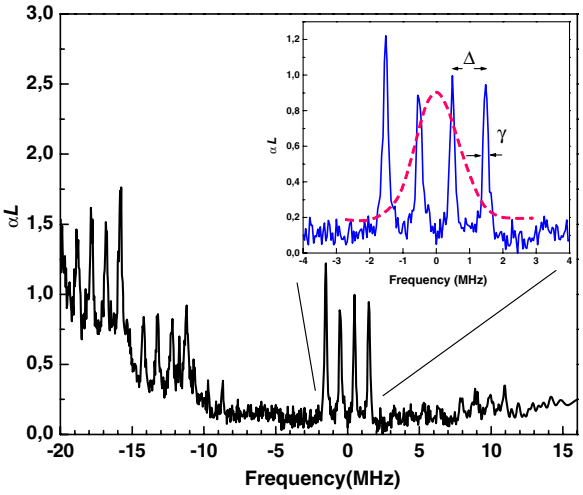

FIG. 3 (color online). The absorption profile created through the optical pumping process is shown. This measurement is done in a small part of the cavity crystal where the coating was removed. From the Pr inhomogeneous absorption profile, four AFC peaks, all absorbing on the $|\pm\frac{5}{2}g\rangle \mapsto |\pm\frac{5}{2}e\rangle$ transition, are created. The spectral content of the storage pulse is shown schematically in the inset by the red dashed line across the AFC structure, which has peak width γ and peak separation Δ. The finesse of the AFC structure is $F_{\mathrm{AFC}} = \frac{\Delta}{\gamma}$.

using a weak readout beam that is frequency chirped at a rate of 10 kHz/μs across the frequency region of the AFC structure. The overall spectral structure is complicated and a detailed discussion of the spectrum is beyond the scope of the present Letter. The inset in Fig. 3 shows the spectral content of the storage pulse relative to the four AFC peaks. The cavity transmission linewidth is tuned to be at least as wide as the whole prepared AFC structure [34]. In this case it was ≈ 11 MHz wide.

The input pulse is stored using the $|\pm\frac{5}{2}g\rangle \mapsto |\pm\frac{5}{2}e\rangle$ transition for ions initially in state $|\pm\frac{5}{2}g\rangle$. A Gaussian pulse with a duration of $\tau_{\mathrm{FWHM}} = 250$ ns and small pulse area is employed as a storage pulse. The frequency of the storage pulse is tuned to the center frequency of an AFC structure with a peak separation $\Delta = 0.9$ MHz. The retrieved echo pulse is detected at detector PD3 after 1.1 μs as shown with black solid line in Fig. 4. In addition, multiple echoes are detected at times 2.2 μs and 3.3 μs which are probably due to multiple rephasing of the ensemble.

In order to assess the storage and retrieval efficiency, the intensity of the input storage pulse at the cavity crystal should be measured. To this end, the cavity crystal was turned $\sim 180°$ such that the input storage pulse impinged on the $R2 = 99.7\%$ mirror, with no pit and peak creation active. In this way the input storage pulse is (almost completely) reflected and the signal on PD3, after calibrating using PD1, can be used as a reference value for the storage pulse input intensity, as shown by a red dashed line in Fig. 4. The pulse area of the first echo at $\approx 1.1\ \mu$s

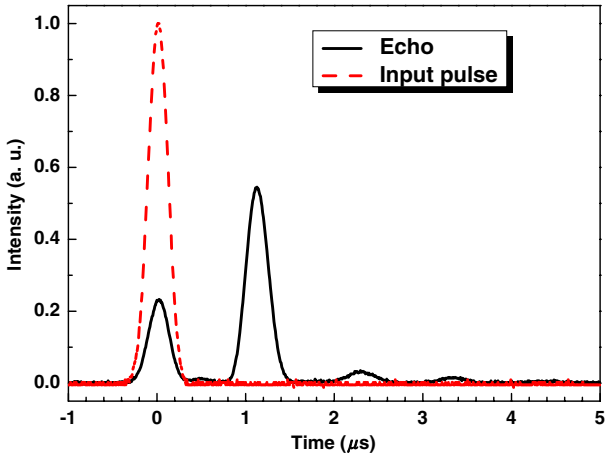

FIG. 4 (color online). The input storage pulse as a reference detected at PD3 (see text) is shown as a red dashed line. The retrieved echo pulse is detected at detector PD3 after 1.1 μs as shown with the black solid line. The area of the echo pulse at 1.1 μs divided by the reference signal pulse area gives a storage and retrieval efficiency of the memory of $\eta = 56\%$.

divided by the reference signal pulse area gives a storage and retrieval efficiency of the memory of $\eta = 56\%$ (four independent measurements gave values ranging from 55.5% to 56.8%). The leakage through the cavity detected on PD2 (see Fig. 1) during the storage is almost negligible ($\approx 1\%$ of the storage pulse).

The present result is lower than the best storage and retrieval efficiency achieved elsewhere [9,10]; however, it is the highest storage and retrieval efficiency based on the AFC protocol, which is presently the best multimode quantum state storage protocol [40], also in the cavity configuration [31]. The source of losses in the current setup can be estimated as about 16% related to the impedance mismatching, 5% associated with the multiple echoes, about 1% from transmission through the cavity, about 10% linked to the AFC finesse dephasing factor, and the rest possibly related to the crystal background absorption. By addressing these losses the efficiency could be improved. We estimate that the efficiency under the same conditions as in this experiment for a crystal in a single-pass configuration would be $<1\%$ [34]. Therefore the cavity configuration shows a significant enhancement compared to the bare crystal.

In order to obtain on-demand and long-term storage based on the AFC protocol [22], the ground-excited state superposition should be transferred to, and then brought back from, a spin-level superposition between two of the ground states [41]. The dephasing due to the spin state inhomogeneous broadening can be suppressed using radio-frequency (rf) spin-echo techniques. In addition, even longer (> 60s) storage time is possible by utilizing zero first-order Zeeman (ZEFOZ) shift [42] and spin-echo techniques to suppress slow variations of the spin transition frequencies [11,12]. Quantum memories in a smaller physical volumes requires significantly lower rf power. Although the present result is 13% lower than the highest rare-earth crystal efficiency results so far [10], it is obtained in a crystal that is 10 times shorter. This may in practice significantly simplify long time, high efficiency spin storage, since too large volumes will require excessive rf powers to compensate for the spin inhomogeneous broadening. In addition, efficient quantum memories in a weakly absorbing media opens up the possibility of utilizing materials with low optical depth but good coherence properties (e.g., Eu^{3+}:Y_2SiO_5 [43]).

In summary, we have demonstrated a quantum memory with $\eta = 56\%$ storage and retrieval efficiency based on the AFC protocol. This is done in a weakly absorbing medium and short crystal length (2 mm) by utilizing an impedance-matched cavity configuration. This achievement, in addition to the storage and recall of weak coherent optical pulses [14,44], spin-wave storage demonstration [41], the best multimode quantum memory [13,14], and storage of entanglement [15,45] increases the possibility of creating an efficient, on-demand, long storage time, and multimode quantum memory based on the AFC protocol in the future.

This work was supported by the Swedish Research Council, the Knut & Alice Wallenberg Foundation, the Maja & Erik Lindqvists forskningsstiftelse, the Crafoord Foundation, and the EC FP7 Contract No. 247743 (QuRep) and (Marie Curie Action) REA Grant No. 287252 (CIPRIS).

[1] K. Hammerer, A. S. Sorensen, and E. S. Polzik, Rev. Mod. Phys. **82**, 1041 (2010).
[2] L. M. Duan, M. D. Lukin, J. I. Cirac, and P. Zoller, Nature (London) **414**, 413 (2001).
[3] N. Sangouard, C. Simon, B. Zhao, Y. A. Chen, H. de Riedmatten, J. W. Pan, and N. Gisin, Phys. Rev. A **77**, 062301 (2008).
[4] P. Kok, W. J. Munro, K. Nemoto, T. C. Ralph, J. P. Dowling, and G. J. Milburn, Rev. Mod. Phys. **79**, 135 (2007).
[5] E. Knill, R. Laflamme, and G. J. Milburn, Nature (London) **409**, 46 (2001).
[6] J. Nunn, N. K. Langford, W. S. Kolthammer, T. F. M. Champion, M. R. Sprague, P. S. Michelberger, X. M. Jin, D. G. England, and I. A. Walmsley, arXiv:1208.1534v1 [Phys. Rev. Lett. (to be published)].
[7] S. Chen, Y.-A. Chen, T. Strassel, Z.-S. Yuan, B. Zhao, J. Schmiedmayer, and J.-W. Pan, Phys. Rev. Lett. **97**, 173004 (2006).
[8] A. I. Lvovsky, B. C. Sanders, and W. Tittel, Nat. Photonics **3**, 706 (2009).
[9] M. Hosseini, B. M. Sparkes, G. Campbell, P. K. Lam, and B. C. Buchler, Nat. Commun. **2**, 174 (2011).
[10] M. P. Hedges, J. J. Longdell, Y. Li, and M. J. Sellars, Nature (London) **465**, 1052 (2010).
[11] J. J. Longdell, E. Fraval, M. J. Sellars, and N. B. Manson, Phys. Rev. Lett. **95**, 063601 (2005).
[12] G. Heinze *et al.* (to be published).

[13] M. Bonarota, J. L. Le Gouët, and T. Chanelière, New J. Phys. **13**, 013013 (2011).
[14] I. Usmani, M. Afzelius, H. de Riedmatten, and N. Gisin, Nat. Commun. **1**, 12 (2010).
[15] E. Saglamyurek, N. Sinclair, J. Jin, J. A. Slater, D. Oblak, F. Bussieres, M. George, R. Ricken, W. Sohler, and W. Tittel, Nature (London) **469**, 512 (2011).
[16] M. Fleischhauer and M. D. Lukin, Phys. Rev. Lett. **84**, 5094 (2000).
[17] K. F. Reim, J. Nunn, V. O. Lorenz, B. J. Sussman, K. C. Lee, N. K. Langford, D. Jaksch, and I. A. Walmsley, Nat. Photonics **4**, 218 (2010).
[18] S. A. Moiseev and S. Kröll, Phys. Rev. Lett. **87**, 173601 (2001).
[19] M. Nilsson and S. Kröll, Opt. Commun. **247**, 393 (2005).
[20] B. Kraus, W. Tittel, N. Gisin, M. Nilsson, S. Kröll, and J. I. Cirac, Phys. Rev. A **73**, 020302 (2006).
[21] G. Hetet, J. J. Longdell, M. J. Sellars, P. K. Lam, and B. C. Buchler, Phys. Rev. Lett. **101**, 203601 (2008).
[22] M. Afzelius, C. Simon, H. de Riedmatten, and N. Gisin, Phys. Rev. A **79**, 052329 (2009).
[23] N. B. Phillips, A. V. Gorshkov, and I. Novikova, Phys. Rev. A **78**, 023801 (2008).
[24] A. Amari, A. Walther, M. Sabooni, M. Huang, S. Kröll, M. Afzelius, I. Usmani, B. Lauritzen, N. Sangouard, H. de Riedmatten, and N. Gisin, J. Lumin. **130**, 1579 (2010).
[25] J. M. Raimond, M. Brune, and S. Haroche, Rev. Mod. Phys. **73**, 565 (2001).
[26] Y. Colombe, T. Steinmetz, G. Dubois, F. Linke, D. Hunger, and J. Reichel, Nature (London) **450**, 272 (2007).
[27] A. V. Gorshkov, A. Andre, M. D. Lukin, and A. S. Sorensen, Phys. Rev. A **76**, 033804 (2007).
[28] B. Julsgaard, J. Sherson, J. I. Cirac, J. Fiurasek, and E. S. Polzik, Nature (London) **432**, 482 (2004).
[29] J. Simon, H. Tanji, J. K. Thompson, and V. Vuletic, Phys. Rev. Lett. **98**, 183601 (2007).
[30] M. Afzelius and C. Simon, Phys. Rev. A **82**, 022310 (2010).
[31] S. A. Moiseev, S. N. Andrianov, and F. F. Gubaidullin, Phys. Rev. A **82**, 022311 (2010).
[32] R. W. P. Drever, J. L. Hall, F. V. Kowalski, J. Hough, G. M. Ford, A. J. Munley, and H. Ward, Appl. Phys. B **31**, 97 (1983).
[33] D. R. Leibrandt, M. J. Thorpe, M. Notcutt, R. E. Drullinger, T. Rosenband, and J. C. Bergquist, Opt. Express **19**, 3471 (2011).
[34] M. Sabooni, S. T. Kometa, S. Thuresson, A. Kröll, and L. Rippe, arXiv:1212.3774 [New J. Phys. (to be published)].
[35] A. Walther, A. Amari, S. Kröll, and A. Kalachev, Phys. Rev. A **80**, 012317 (2009); Correction: the expression for the group velocity needs to be corrected to $v_g = \frac{2\pi\Gamma}{\alpha}$ in subsection "IV.B. Slow light effects."
[36] M. Sabooni *et al.* (in preparation).
[37] A. E. Siegman, *Lasers* (University Science Books, Mill Valley, California, 1985).
[38] L. Rippe, M. Nilsson, S. Kröll, R. Klieber, and D. Suter, Phys. Rev. A **71**, 062328 (2005).
[39] M. Nilsson, L. Rippe, S. Kröll, R. Klieber, and D. Suter, Phys. Rev. B **70**, 214116 (2004); M. Nilsson, L. Rippe, S. Kröll, R. Klieber, and D. Suter, Phys. Rev. B **71**, 149902 (E) (2005).
[40] J. Nunn, K. Reim, K. C. Lee, V. O. Lorenz, B. J. Sussman, I. A. Walmsley, and D. Jaksch, Phys. Rev. Lett. **101**, 260502 (2008).
[41] M. Afzelius, I. Usmani, A. Amari, B. Lauritzen, A. Walther, C. Simon, N. Sangouard, J. Minar, H. de Riedmatten, N. Gisin, and S. Kröll, Phys. Rev. Lett. **104**, 040503 (2010).
[42] M. Lovric, P. Glasenapp, D. Suter, B. Tumino, A. Ferrier, P. Goldner, M. Sabooni, L. Rippe, and S. Kröll, Phys. Rev. B **84**, 104417 (2011).
[43] B. Lauritzen, N. Timoney, N. Gisin, M. Afzelius, H. de Riedmatten, Y. Sun, R. M. Macfarlane, and R. L. Cone, Phys. Rev. B **85**, 115111 (2012).
[44] M. Sabooni, F. Beaudoin, A. Walther, N. Lin, A. Amari, M. Huang, and S. Kröll, Phys. Rev. Lett. **105**, 060501 (2010).
[45] C. Clausen, I. Usmani, F. Bussieres, N. Sangouard, M. Afzelius, H. de Riedmatten, and N. Gisin, Nature (London) **469**, 508 (2011).
[46] Y. C. Sun, *Spectroscopic Properties of Rare-Earths in Optical Materials* edited by G. Liu and B. Jacquier, Springer Series in Material Science (Springer, Berlin Heidelberg, 2005), Chap. 7.